



**jwst**



**esa**

**STScI**

JWST Science & Operations Centre  
3700 San Martin Drive  
Baltimore MD 21218  
USA

[www.esa.int](http://www.esa.int)

# DOCUMENT

## Generating pre-flight path loss reference files from simulations

<b>Prepared by</b>	<b>E. Puga</b>
<b>Reference</b>	<b>ESA-JWST-SCI-NRS-TN-2019-004</b>
<b>Issue/Revision</b>	<b>1.0</b>
<b>Date of Issue</b>	<b>June 9, 2020</b>
<b>Status</b>	<b>Draft</b>



# APPROVAL

<b>Title</b> Generating pre-flight path loss reference files from simulations	
<b>Issue Number</b> 1	<b>Revision Number</b> 0
<b>Author</b> E. Puga	<b>Date</b> June 9, 2020
<b>Approved by</b>	<b>Date of Approval</b>
M. Sirianni	

# CHANGE LOG

Reason for change	Issue Nr.	Revision Number	Date

# CHANGE RECORD

<b>Issue Number</b> 1	<b>Revision Number</b> 0		
Reason for change	Date	Pages	Paragraph(s)

# DISTRIBUTION

Name/Organisational Unit
SCI-ODJ
STScI



## Contents

<b>1 Introduction</b>	<b>4</b>
1.1 Path loss map simulations . . . . .	4
1.1.1 Generation of exploratory simulations . . . . .	4
1.1.2 Optimal aperture sampling determination for simulations . . . . .	5
1.1.3 Final simulations Generation . . . . .	8
1.2 Path loss correction algorithms . . . . .	11
1.2.1 FS and MOS . . . . .	12
1.2.2 IFS . . . . .	14
1.3 Path loss reference file generation . . . . .	14
1.4 Path loss reference file format . . . . .	14
1.5 Path loss correction application . . . . .	15
<b>2 Conclusion</b>	<b>15</b>
<b>Appendices</b>	<b>16</b>
<b>A IFS Response</b>	<b>16</b>

## 1 INTRODUCTION

The radiometric calibration of the NIRSpec instrument is tied to the observations of spectrophotometric standard stars for each mode of observation. This initial calibration will only be valid for a point source centred in a NIRSpec aperture (micro-shutter pseudo-slit, slice or slit). As summarized in [ESA-JWST-SCI-NRS-NTN-2019-003: The in-orbit radiometric calibration of the NIRSpec instrument](#), additional corrections need to be introduced to account for non-centred point-like sources or for sources that are not point like. In the following, we will only consider the case of sources that fully illuminate the aperture in a uniform fashion (i.e. uniformly extended sources).

The path loss is a correction to the radiometric calibration that include two different light loss sources linked to the use of apertures: the geometrical loss due to the truncation of the PSF by a finite aperture in the image plane and the diffraction loss component, which corresponds to light diffracted by the aperture borders that will not make it through the pupil, resulting in the sculpting of the pupil illumination function.

The presently described reference files are tailored to the algorithm in the data calibration pipeline, and derived from the analysis of the simulated cubes.

### 1.1 Path loss map simulations

The construction of the pre-flight reference files relies on simulated path loss maps, previously generated using a Python model of the radiometric response of the NIRSpec instrument. The `psf` family scripts calculate the efficiency of the optical elements using the NIRSpec geometrical and NIRSpec + OTE Fourier Optics models. The Matrix Fourier Transform method relies on a matrix-based computation of the discrete Fourier transforms developed by R. Soummer et al. for applications of Fourier-optics calculations to coronagraphy. This method results in more efficient calculations using smaller sized matrices, as it removes the link in sampling and size between image and pupil planes. It also limits the computation to the unmasked areas. This functionality is provided in the Python package `poppy`.

#### 1.1.1 Generation of exploratory simulations

The Python PSF family scripts compute point-spread functions and pupil illumination in various instrument planes. The simulated path loss maps of the integrated light are obtained by moving a point source in a grid across the aperture. These, are then used to obtain the geometrical and diffraction loss components at the aperture and GWA plane, which are the ingredients to derive the correction for path loss.

The script `mp_psf.py` (for MOS, FS) within `nrspsim.psf` is used to create the loss maps for the geometrical and diffraction components. It requires a configuration file as input with the necessary prescriptions regarding:

- configuration,
- NIRSpec geometrical model and OTE + instrument Fourier Optics model,
- parameters of extent/size and sampling of the various optical planes

The reference system in the aperture plane is tied to the central point of each aperture and relative to its size (FS, IFS) or shutter pitch (MOS), in both x and y dimensions. In the following, the convention for number of sampling grid points (`nw`, `nx`, `ny`) is denoted with the nomenclature `W_X_Y`, used to name the directories. The spatial extent of a generic simulation is typically the aperture size range `[-0.5, 0.5]`, but may extend further away in one or various spatial dimensions (e.g. y-dimension for the 3 shutter slitlet). The wavelength extent is typically the range `[0.6-6.0]`  $\mu\text{m}$ , which corresponds to the spectrograph instantaneous coverage.

The batch generation of families of simulations for the NIRSpec apertures (FS200A1, FS400A1, FS1600A1, MOS1x1, IFS) is performed with `pthl_create_simulations.py`. It generates the directory tree structure, modifies a default input `.json` file (named `pthlSimu.json`) and runs the simulations, creating an output configuration file and the geometric and diffraction loss cubes. This is obtained running

```
python pthl_create_simulations.py /Users/epuga/JWST_NIRSpec/NIRSpec_Calibration/PathLoss/Simulations/
jpro_PthlSampling_Q1_varX pthlSim.json
```

Observing Aperture	Aperture oversampling		Pupil Oversampling		Error
	nx	ny	nx	ny	
FS1600A1	800	800	800	800	0.0001%
FS200A1	400	800	800	800	0.10%
FS200A2	400	800	800	800	0.10%
FS200B1	400	800	800	800	0.10%
FS400A1	800	800	800	800	0.10%
MOS1x1	400	800	800	800	0.50%
MOS1x3	400	800	800	800	0.50%
IFS	200	800	800	800	0.10%

Table 1: Optimal aperture and pupil sampling.

FS, MOS, IFS - Q1 simulations		
W.X.Y		
Varying W	Varying X	Varying X.Y
5_3_3	5_5_25	5_5_5
11_3_3	5_11_25	5_11_11
21_3_3	5_15_25	5_15_15
31_3_3	5_25_25	5_25_25
51_3_3	5_51_25	5_51_51

Table 2: Path loss sampling simulations in one quarter of the aperture. The finest sampling grid (reference) is shown in red.

**Note**

The most up-to-date version of this script (which includes also IFS) is in a PyCharm project in JPRO.

### 1.1.2 Optimal aperture sampling determination for simulations

A series of tests were run with different values for the sampling of the aperture (MSA) and pupil (GWA) planes and reported in [ESA-JWST-SCI-NRS-HO\\_2018-001: nrspysim.psf pathloss & PSF computation. Nominal computation parameters](#). The resulting parameters detailed in Table 1 ensure an uncertainty of a fraction of a percent.

For the analysis of the loss map downsampling effects, the exploration of sampling grids was performed in either spatial or wavelength dimension. The directory of simulations for one or two sampling grid values called **sampling family** and uses the wildcard symbol on the variable grid point dimension(s) (e.g. \*\_03\_03). The spatial extent corresponds to one quarter of the aperture [0.0, 0.5] for both x and y for FS and IFS, and [0.0, 0.36] for x and y for MOS.

In each simulation family, we follow a bottom-up strategy for simulation generation to minimize computation time, performing our sampling interpolation error analysis as we increase the sampling grid (see Table 2).

The method to estimate the downsampling interpolation error metric consists of:

- resampling the coarser path loss simulated cubes ( $G_k$  and  $D_k$ ) in a simulation family to the finest sampling simulated cube (considered infinitely sampled)
- $(w_i, x_i, y_i)$  grid of reference points  $\rightarrow G_i, D_i$

- $(w_i, x'_i, y'_i)$  grid of spatially interpolated points  $\rightarrow G'_i, D'_i$
- $(w'_i, x_i, y_i)$  grid of spectrally interpolated points  $\rightarrow G'_i, D'_i$
- calculating the difference of each with respect to the finest sampling cube
- estimate of the standard deviation of difference in either wavelength or spatial dimensions for each geometrical and diffraction losses. This is considered path loss map accuracy on absolute flux for that coarse sampling.

We use a downsampling error convergence criteria below the path loss absolute flux error budget (5% for FS and MOS, 2% for IFS) of 1% for all modes and apertures.

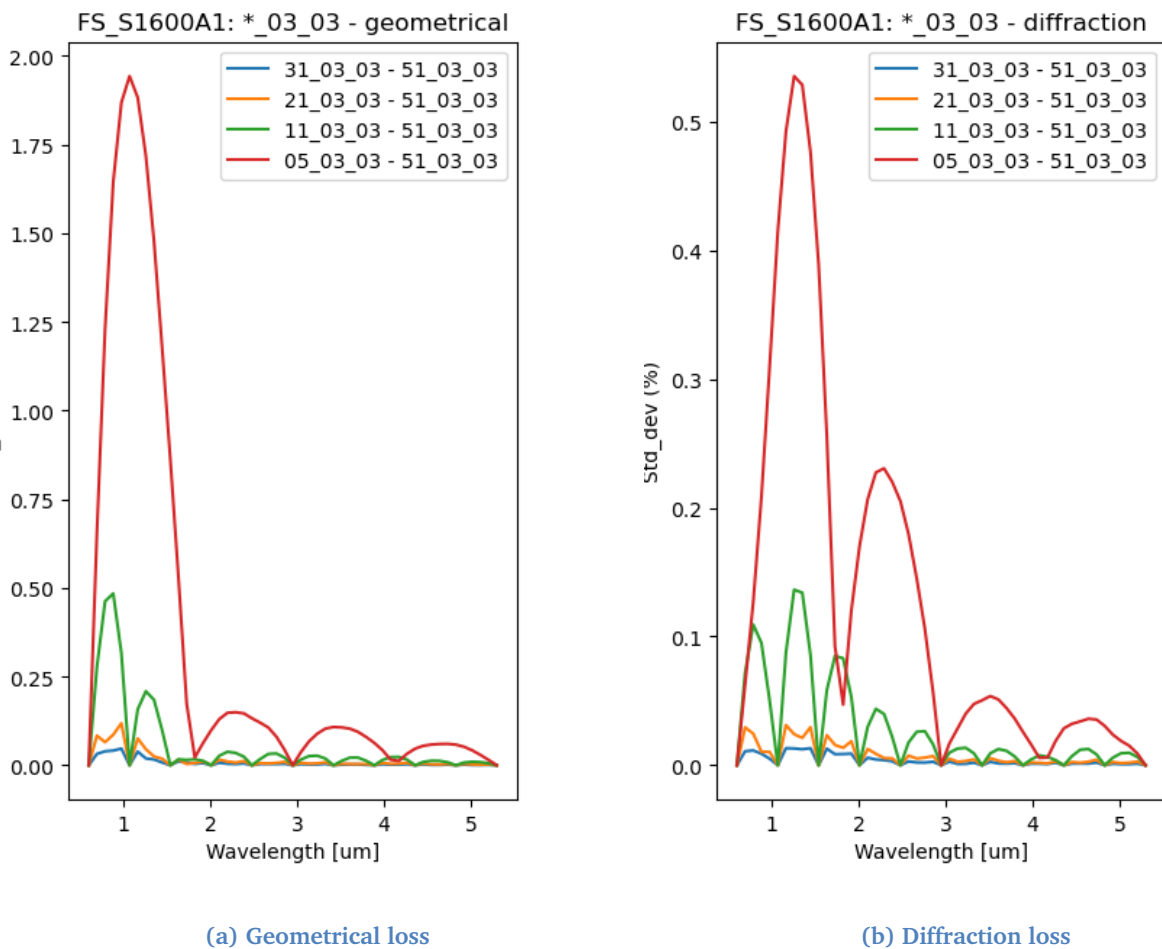


Figure 1: FS1600A1: Standard deviation of difference between reference and interpolated coarser-grid sampling family

**Note**

- The merit function for the error budget is the  $1\sigma$  RMS 5% for FS and MOS factors two contributions:
- o The standard deviation of path loss accuracy over the aperture (acceptance zone) including zero difference values due to common sampling points of sampling grids.
  - o The error from the target acquisition finite accuracy (This has been previously described in CRAL-PJT-NIRS-TN-200503-03, but only calculated for the spectral direction and expressed as maximum absolute flux accuracy). The information missing is the spatial direction and the standard deviation over the aperture (or selected area in the aperture)



Aperture	MAX(STD[*_3_3-51_3.3])<0.5%		MAX(STD[*_25-5.51_25]), ΔSTD [(25-15), (15-11), (11-5)]		MAX(STD[5_*_-5_51_51])	
	Geometrical	Diffraction	Geometrical	Diffraction	Geometrical	Diffraction
FS1600A1	0.48 (11)	0.14 (11)	0.47 (25)	[+0.8, +1.37, +5.16]	0.62 (25_25)	0.17 (25_25)
FS200A1	0.38 (21)	0.08 (21)	0.03 (25)	[+0.05, +0.07, +0.44]	0.56 (25_25)	0.25 (25_25)
FS400A1	0.63 (11)	0.21 (11)	0.08 (25)	[+0.13, +0.13, +1.69]	0.69 (25_25)	0.24 (25_25)
MOS1x1	0.18 (21)	0.22 (21)	0.14 (15)	[+0.09, +0.13, +1.06]	0.30 (15_15)	0.21 (15_15)
IFS	0.29 (21)	0.11 (21)	<0.01 (25)	[+0.02, +0.02, +0.28]	0.55 (25_25)	0.30 (25_25)

Table 3: Maximum standard deviation of the interpolation error (in absolute flux percentage) in a simulated family, varying the sampling parameters in W, X and Y dimensions. Optimal sampling determination is estimated first over the W dimension and then over the X dimension, in which the geometrical loss dominates. MOS1x3 optimal sampling is a scaled version of MOS1x1.

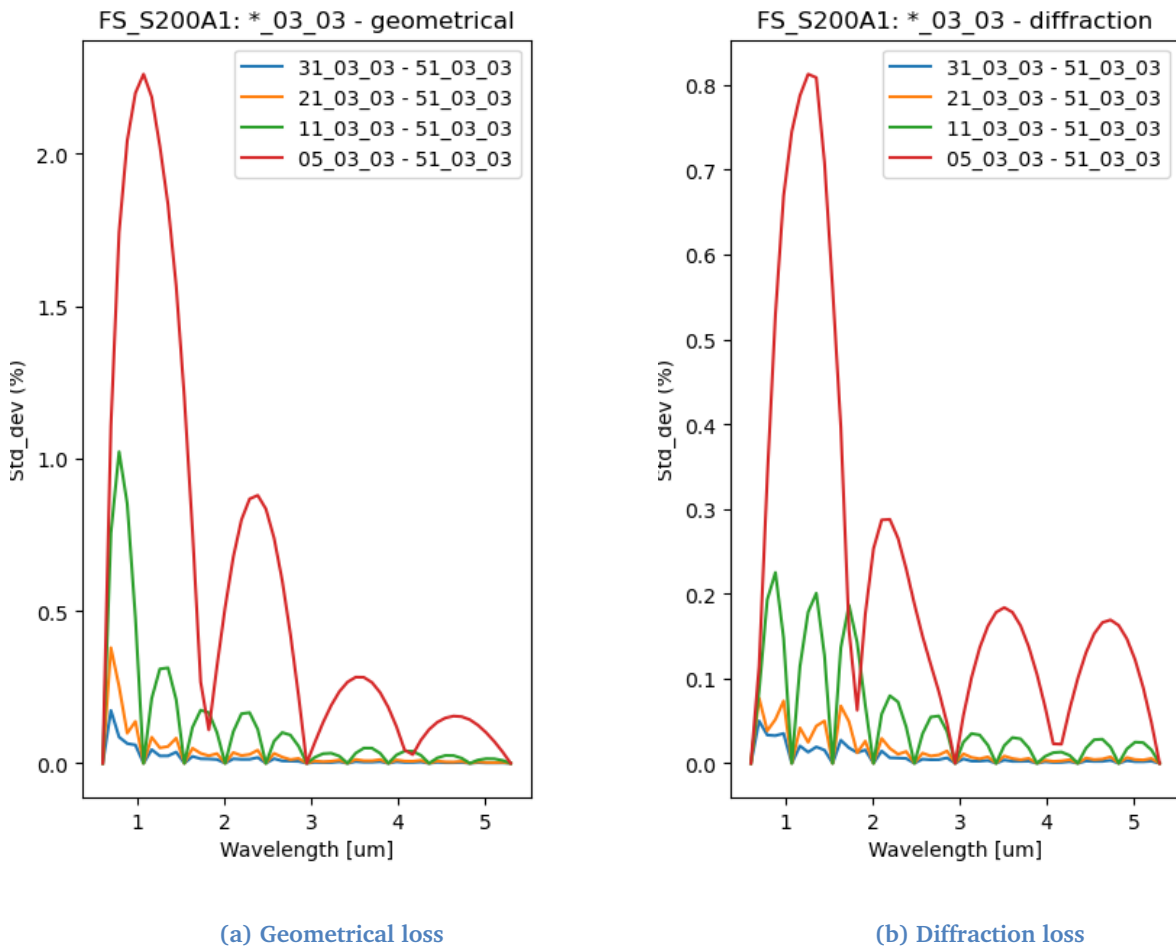


Figure 2: FS200A1: Standard deviation of difference between reference and interpolated coarser-grid sampling family

This analysis does **not** include:

- o The product of the geometrical and diffraction efficiencies (1-G)·(1-D)
- o Scipy RectBivariateSplines interpolation algorithm as path loss reference file class uses the griddata (linear) algorithm.

In Table 3, the selected optimal grid parameters selected that amount an uncertainty of less than 0.7% for both the geometrical and diffraction losses. For the X dimension, we provide the increment in uncertainty between the coarser families.

### 1.1.3 Final simulations Generation

The final bundle of simulations with the determined optimally sampled parameters for the three observing modes and the various apertures comprise:

- coarse grid simulations over the extent of the aperture for point-like sources.
- fine grid simulations used as reference for downsampling error estimate.
- (coarse grid) oversized simulations for the uniformly extended sources.

Table 4 summarizes the extent and sampling of the necessary path loss maps.



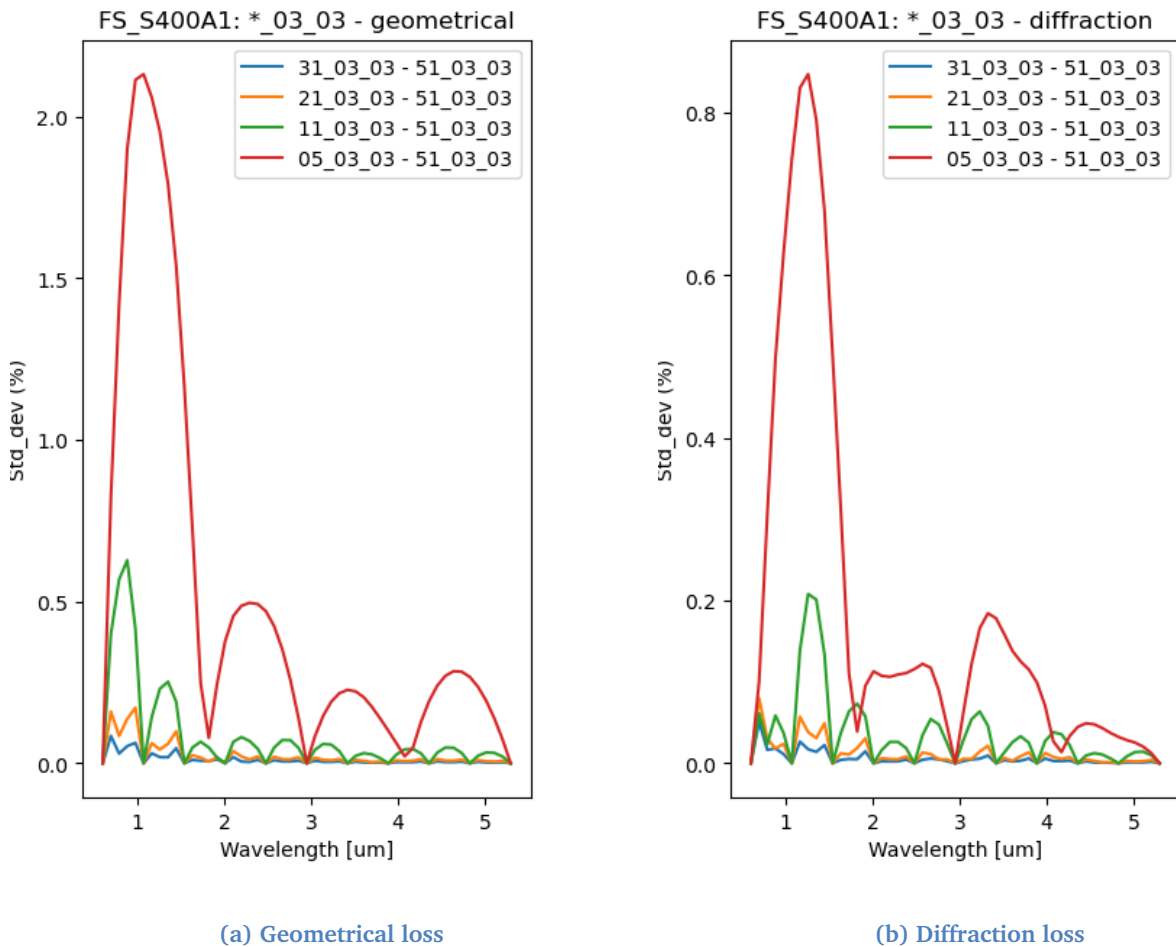


Figure 3: FS400A1: Standard deviation of difference between reference and interpolated coarser-grid sampling family

The generation of these files is performed with the following command:

```
python pthl_create_simu_json.py /Users/epuga/JWST_NIRSpec/NIRSpec_Calibration/PathLoss/Simulations/error_Pthl pthlSim.json
```

The downsampling error is currently calculated only for the point-like source extension (i.e. using simulations over the aperture extent and not in the oversized version of the simulations). The algorithm calculates the residuals between the interpolated coarse grid sampling pathloss cube and the fine grid sampling pathloss cube (reference). The uncertainty in the loss is calculated as the 3D Integral of the residuals. In this approach, we null the weight of common nodes and non-zero projected distance in the point source location with respect to the simulations sampling grid.

**Warning**

The integral is calculated in a flattened structure, therefore successive reductions in size are used in the code. This might be changed to a masking scheme like the one used in the reference file generation to preserve the cube structure and facilitate the result visualization. This routine is only tested with "spot checks".

The generation of the error maps is a preliminary step to generating the path loss reference files. This is achieved

Aperture	Nominal		Reference		Oversized	
	Bounds (X, Y)	Grid (W, X, Y)	Bounds (X, Y)	Grid (W, X, Y)	Bounds (X, Y)	Grid (W, X, Y)
FSI600A1	[-0.5, 0.5], [-0.5, 0.5]	(11, 51, 51)	[-0.5, 0.5], [-0.5, 0.5]	(31, 101, 101)	[-1., 1.], [-1., 1.]	(11, 101, 101)
FS200A1	[-0.5, 0.5], [-0.5, 0.5]	(21, 51, 51)	[-0.5, 0.5], [-0.5, 0.5]	(31, 101, 101)	[-1., 1.], [-1., 1.]	(21, 101, 101)
FS200A2	[-0.5, 0.5], [-0.5, 0.5]	(21, 51, 51)	[-0.5, 0.5], [-0.5, 0.5]	(31, 101, 101)	[-1., 1.], [-1., 1.]	(21, 101, 101)
FS200B1	[-0.5, 0.5], [-0.5, 0.5]	(21, 51, 51)	[-0.5, 0.5], [-0.5, 0.5]	(31, 101, 101)	[-1., 1.], [-1., 1.]	(21, 101, 101)
FS400A1	[-0.5, 0.5], [-0.5, 0.5]	(11, 51, 51)	[-0.5, 0.5], [-0.5, 0.5]	(31, 101, 101)	[-1., 1.], [-1., 1.]	(11, 101, 101)
MOSIX1	[-0.5, 0.5], [-0.5, 0.5]	(21, 31, 31)	[-0.5, 0.5], [-0.5, 0.5]	(31, 101, 101)	[-1., 1.], [-1., 1.]	(21, 61, 61)
MOSIX3	[-0.5, 0.5], [-1.5, 1.5]	(21, 31, 91)	[-0.5, 0.5], [-1.5, 1.5]	(31, 101, 277)	[-1., 1.], [-1.733, 1.766]	(21, 61, 106)
IFS	[-5.5, 5.5], [-0.5, 0.5]	(21, 551, 51)	[-5.5, 5.5], [-0.5, 0.5]	(31, 1101, 101)	[-5.5, 5.5], [-0.5, 0.5]	(31, 1101, 101)

Table 4: Optimal aperture and pupil sampling.

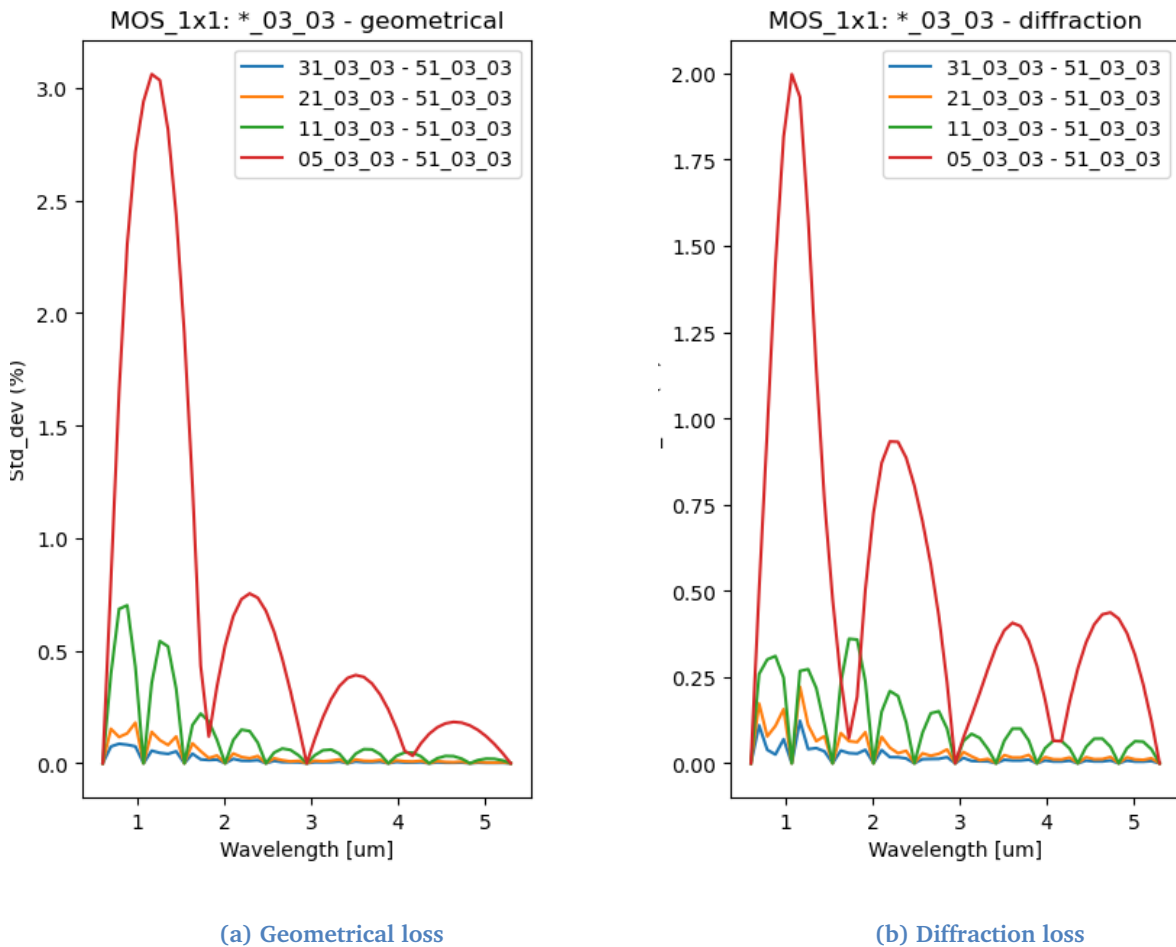


Figure 4: MOS1x1: Standard deviation of difference between reference and interpolated coarser-grid sampling family

running

```
python pthl_interp_error.py /Users/epuga/JWST_NIRSpec/NIRSpec_Calibration/PathLoss/Simulations
```

in the nrspysim package

## 1.2 Path loss correction algorithms

The path loss corrections are constructed for two source types:

**Point sources:** Path loss maps are converted to efficiencies (1 - loss map) and the pixel-by-pixel product of the geometrical and diffraction efficiencies is then normalized to its value at the aperture centre. The correction is therefore relative

**Extended sources:** For uniformly extended sources, the path loss efficiency was approximated by the integral of the system response divided by the slit aperture size, in the spectral dimension, using simulated path loss maps that extend well beyond the limits of the correspondent aperture.

Despite the name "loss", what the reference file contains is an efficiency or response that is

$$\eta_G(dx, dy, \lambda) = 1 - G(dx, dy, \lambda) \tag{1}$$

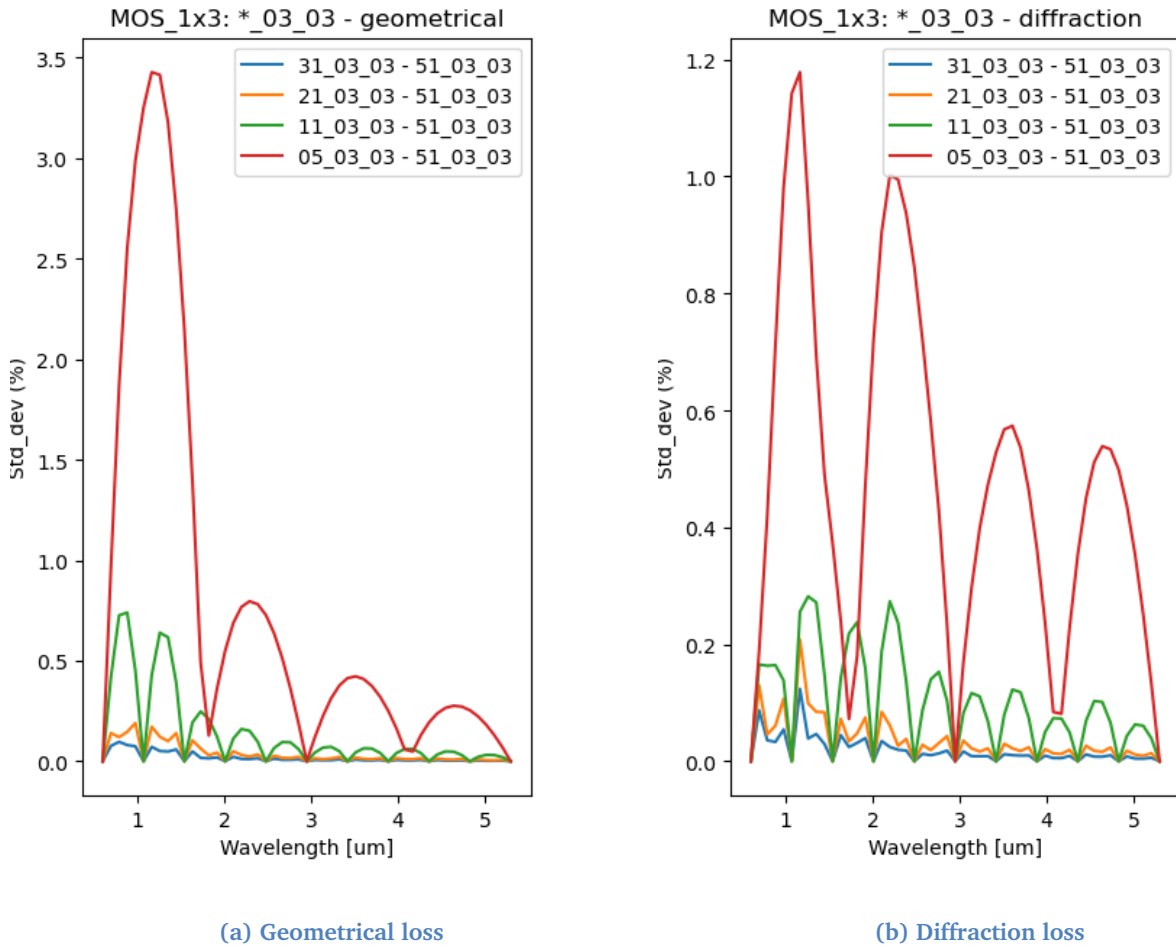


Figure 5: MOS1x3: Standard deviation of difference between reference and interpolated coarser-grid sampling family

The following algorithms are part of the script `pth1_generate.py` in the package `nrspsytools` (for CDP3, the uniformly extended path loss correction algorithm was part of the Class `Pth1Ref` in `nrspsytools.pth1_reference.py`).

### 1.2.1 FS and MOS

The path loss reference file cube for **point-like sources** is constructed from the path loss simulation cubes following:

$$\eta_{PS}(dx, dy, \lambda) = \frac{1}{C_{point}} \cdot (1 - G(dx, dy, \lambda)) \times (1 - D(dx, dy, \lambda)) \quad (2)$$

where

$$C_{point} = (1 - G(0, 0, \lambda)) \times (1 - D(0, 0, \lambda)) \quad (3)$$

G and D are the geometrical and diffraction path loss maps simulated at the wavelengths covered by the PRISM filter. They are defined with respect to the reference system located at the centre of the aperture, relative to the pitch size.  $C_{point}$  corresponds to the value of the path loss at the aperture central position, so that the correction is 1.0 at this position. The path loss efficiency is thus relative to that of a centred point source, which is the reference of NIRSPEC radiometric calibration.

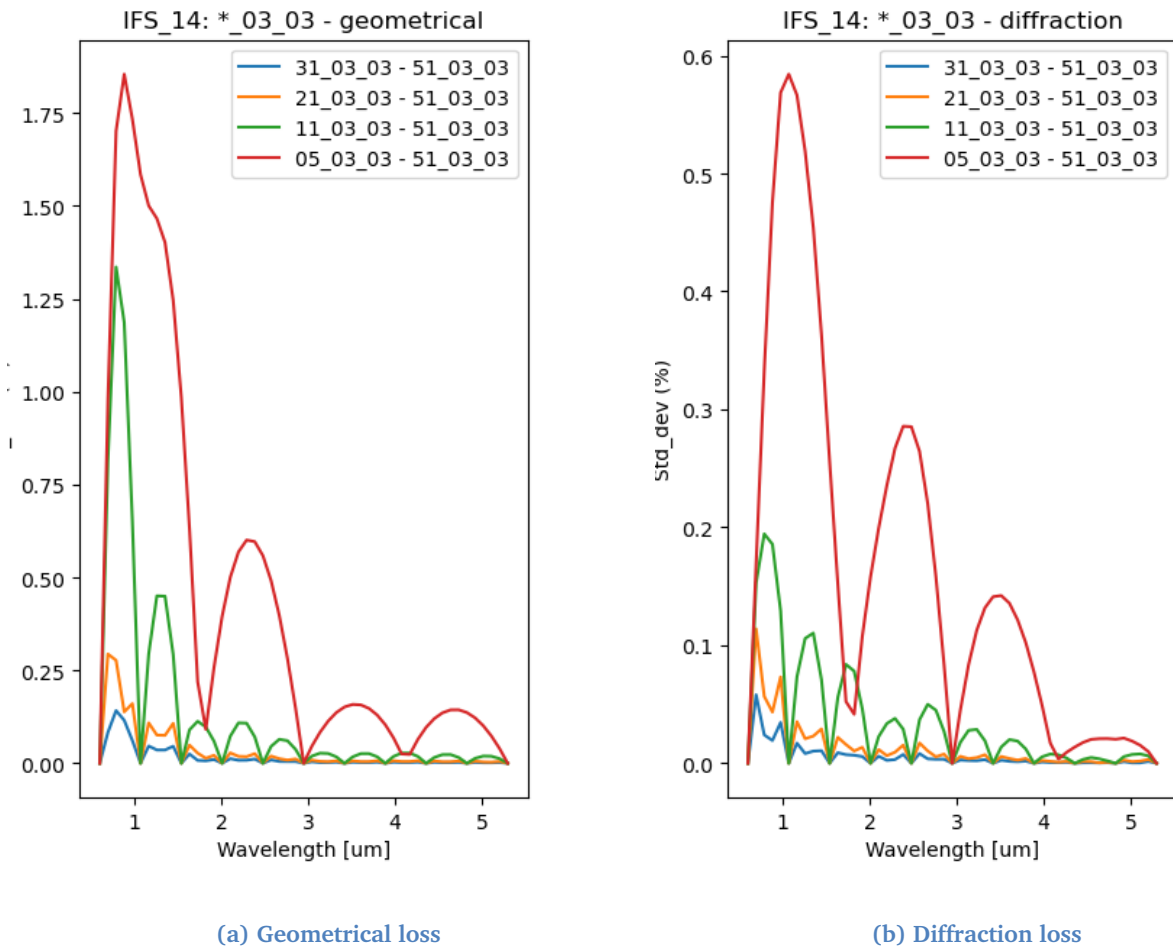


Figure 6: IFS Slice 14: Standard deviation of difference between reference and interpolated coarser-grid sampling family

For **uniformly extended sources**, the one dimensional table is calculated as a weighted sum

$$\eta_{UNI}(\lambda) = \frac{1}{C_{point}} \cdot \frac{\int_{-\infty}^{+\infty} (1 - G(dx, 0, \lambda)) \times (1 - D(dx, 0, \lambda)) dx}{W} \tag{4}$$

$$\approx \frac{1}{C_{point}} \cdot \frac{\sum_{x_{min}}^{x_{max}} \{(1 - G(\delta x, 0, \lambda)) \times (1 - D(\delta x, 0, \lambda))\} \delta x}{W}$$

and  $W$  is the width of the aperture, and equivalent to  $\sum (1 - G) \delta x$ .

### 1.2.2 IFS

The path loss correction for IFS utilizes the response of 11 slices, following the results of Appendix A.

$$\eta_{PS}(dx, dy, \lambda) = \frac{1}{C_{point}} \cdot \frac{1}{\sum_{S=-5}^{+5} (1 - G_{15}(S + dx, dy, \lambda))} \cdot \sum_{S=-5}^{+5} (1 - G_{15}(S + dx, dy, \lambda)) \times (1 - D_{15}(S + dx, dy, \lambda)) \quad (5)$$

and

$$C_{point} = \frac{\sum_{S=-5}^{+5} (1 - G_{15}(S + 0, 0, \lambda)) \times (1 - D_{15}(S + 0, 0, \lambda))}{\sum_{S=-5}^{+5} (1 - G_{15}(S + 0, 0, \lambda))} \quad (6)$$

where  $S$  corresponds to the width of the slice and the evaluation at  $S + dx$  mimics the contribution of the adjacent slice. These contributions span in a range of  $S$   $[-5, +5]$  around the central slice 15.

$$\eta_{UNI}(\lambda) \approx \frac{1}{C_{point}} \cdot \frac{\sum_x \{(1 - G_{15}(\delta x, 0, \lambda)) \times (1 - D_{15}(\delta x, 0, \lambda))\} \delta x}{S} \quad (7)$$

#### Note

The error extension has been populated for point-like sources including only the down-sampling 2D interpolation error. It would be desirable to include Target Acquisition uncertainty and instrument model error. The error extension for uniformly extended sources is not yet calculated (requires a reference too) and it is currently populated with zeros.

Oversized path loss simulations for uniformly extended sources should be more largely oversized. This would not imply larger computation times, as the oversizing is only required in the x-dimension.

## 1.3 Path loss reference file generation

The generation of the path loss reference files is centralized in a unique script that loads the simulated geometrical and diffraction losses and implements the algorithms for path loss correction described in Section 1.2 by running the command

```
nrspytools
```

```
python pthl_generation_script.py ./pthl_config_FS200X.json
```

This needs to be executed for the observing modes and apertures FS1600A1, FS200A1, FS400A1, MOS1x1, MOS1x3 and IFS. In the case of FS200A1, we name the configuration file X as it creates analog reference files for FS200A1, FS200A2 and FS200B1 by setting the configuration file parameter:

```
"force_aperture": ["", "S200A2", "S200B1"]
```

## 1.4 Path loss reference file format

The path loss reference file format follows the description outlined in the CDP3 delivery note [ESA-JWST-SCI-NRS-TN-2016-017: The correction of path losses for uniform and point sources](#). It also incorporates the reference file keyword definitions in [ESA-JWST-SCI-NRS-DD-2017-001: A reference file repository for NIPS](#) and it should be compatible with the architecture of NIPS 2.0. The file `pthl_ref_tools.py` in `nrspytools` contains the refurbished Class for generating the structure, comparison, manipulation, I/O and interpolation utilities that are necessary to create path loss reference files.

`pthl_ref_tools.py` contains the `PthlRefTools` Class, which differs from the original `PthlRef` Class in `pthl_reference.py` in the following aspects:

1. Data structure refurbishment, now in line with NIPS 2.0 Pth1Ref Class: data, error, wcs.
2. `m_set_to_zeros` deprecated, with `m_set` in-line with NIPS 2.0 Pth1Ref to set container.
3. `m_compute_average_correction` merged with `m_compute_correction_uniform`, passing cube as parameter to allow "function-like" usage.
4. Harmonisation across methods to define apertures with attributes `start_xy`, `size_xy/pitch_xy`, storing it in the wcs object.
5. I/O tuned to use wcs object and info therein, instead of header keywords.
6. `m_write_to_fits` and `m_read_from_fits` methods changed to reflect CDP3 reference file format (in the porting to py 3.X, the format was changed back to that of the `nrspylib.radiometry.losses` Class)
7. Change of `m_interpolate_spectral` passing cube as parameters.
8. Change of `m_interpolate_spatial`, `m_interpolate_spectral_spatial` passing cube as parameter.
9. Created `m_eq_wavelength_grid` to interpolate the data and error cubes to an evenly spaced wavelength grid, and respect the reference file structure (wcs).
10. Fixed bug on the `m_interpolate_spectral` which change the interpolated value to `fill_value` if the new wavelength grid included the lower limit of the initial wavelength grid (default).
11. Ad-hoc `m_compare`-style method to compare wcs attributes. Analog included in `nrspylib.utils.compare` in 07/2019.

### Warning

The uncertainties for the point-like and uniformly extended source extensions are expressed in terms of the variance of the path loss correction (PSVAR, UNIVAR). In 2019 this specification was deemed inconsistent with most NIRSpec reference files.

## 1.5 Path loss correction application

The application of the path loss correction is specified in [ESA-JWST-SCI-NRS-NTN-2019-003: The in-orbit radiometric calibration of the NIRSpec instrument](#). The path loss correction for point sources is applied by the pipeline onto the irregular 2D spectrum, as a broadcasted correction in the y-dimension, but it is meant to be meaningful on the final extracted 1d spectrum over the aperture size defined for the spectrophotometric calibration.

## 2 CONCLUSION

The presented reference files differ to those in CDP3 (30/03/2016) in the following:

- The sampling has been optimized so that the downsampling interpolation error is well below the uncertainty budget associated to the path loss correction step.
- IFS path loss correction was a placeholder, both simulations and the reference file computation algorithm needed to be developed
- The uniform source algorithm was approximated by the integral of the system response divided by the slit aperture size. This has been changed to a weighted sum approach.
- We have now populated the PSVAR extension

The software development of this work has been embedded within the packages `nrspysim` and `nrspytools`.

What remains to be revised is the normalization for FS200X and FS400A1, whose dither positions are defined with respect to a corrected central position due to the imperfections in the aperture. These redefined central positions are part of the SIAF configuration file. A potential change of the path loss uncertainty extension from variance to error.

# Appendices

## A IFS RESPONSE

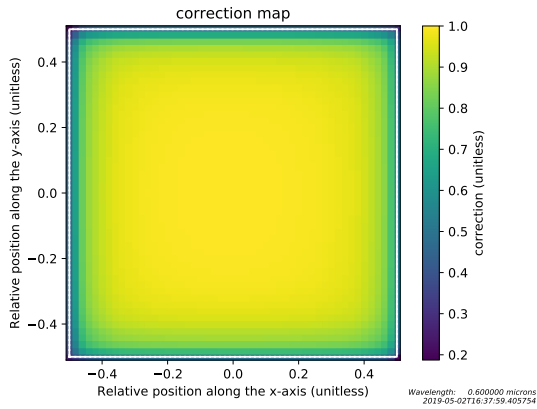
For a point source, most of the flux falls onto a limited number of slices in the dispersion direction. In order to minimize the noise introduced by low-level intensity slices, we try to isolate the number of contributing slices to the instrument response using the geometrical loss simulations to create the integrated efficiency seen by every slice in the NIRSpec IFS. This is calculated for 11 wavelengths in the NIRSpec spectral range [0.6-6.0] microns. Fig. 8 shows that the peak value of the instrument response is the fraction of PSF seen by the central slice, and that fraction decreases with wavelength. In the same figure, it is shown the Encircled Energy Fraction as a function of radius in slices. The horizontal lines represent 95% and 99% of the EEF. Therefore, we could establish that most of the flux falls within a radius of 5 slices in the dispersion direction.

Additionally, Fig. 9 shows the fraction of flux seen by the IFU FoV (including the 30 slices) for a point source centred on the central reference slice #14 with wavelength. The fraction of flux lost outside of the IFU is 5%–10%.

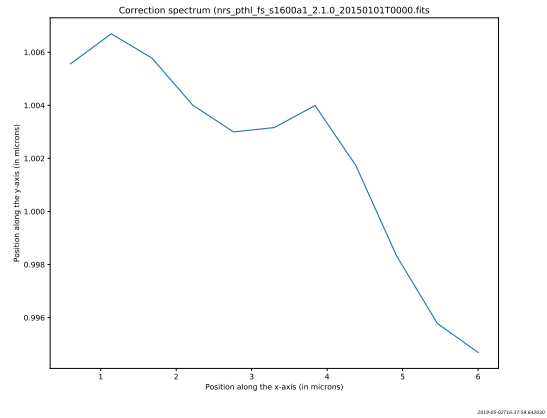
The script for `ifs_ptl_create_simulations.py` loads the simulated maps with one position per aperture, and limits `[xmin, xmax] = [-15.5, 15.5]` to extend over the total of 30 slices in the IFS FoV, and calculates the number of slices for which the geometrical loss has a 95% power included. The calling sequence includes working directory and simulations configuration file

```
python ifs_ptl_create_simulations.py /Users/epuga/JWST_NIRSpec/NIRSpec_Calibration/PathLoss/  
Simulations/test_IFS_Norm IFS_SimJpro.json
```

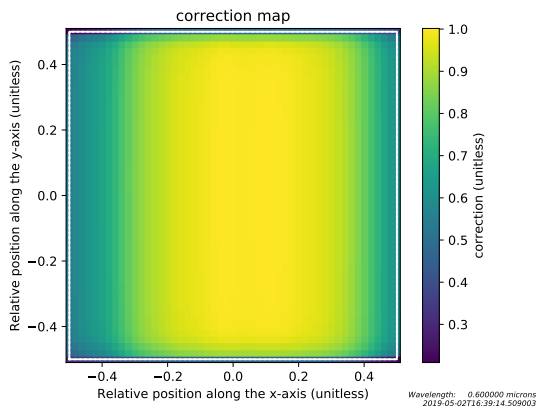




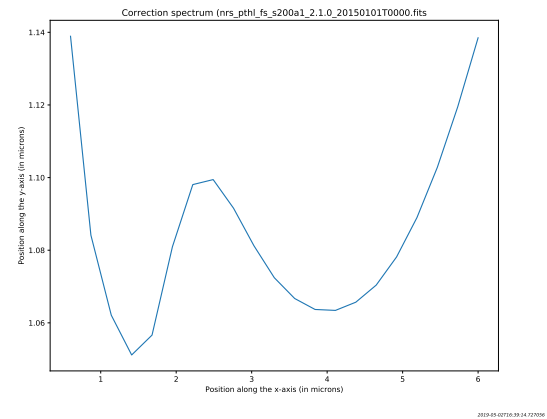
(a) FS1600A1: Point-like source at 0.6  $\mu$  m



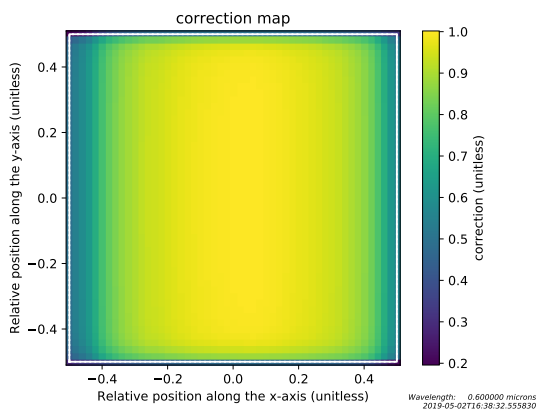
(b) FS1600A1: Uniformly extended source



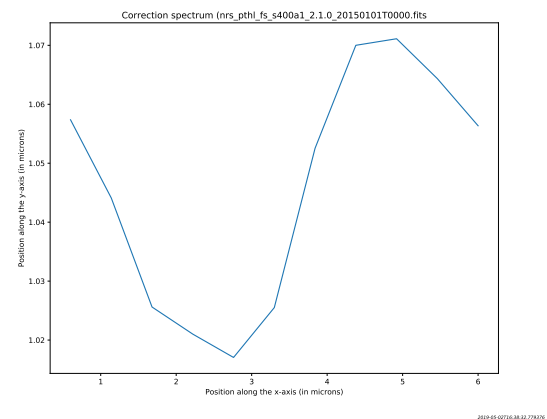
(c) FS200A1: Point-like source at 0.6  $\mu$  m



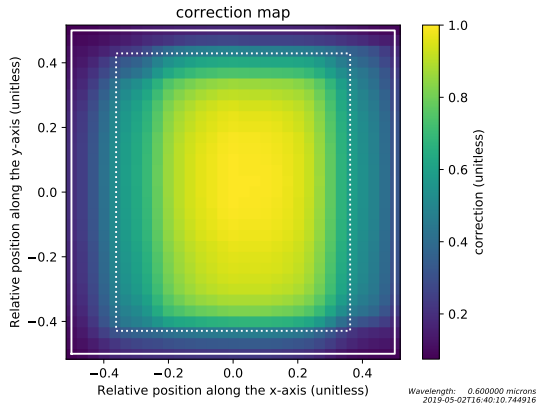
(d) FS200A1: Uniformly extended source



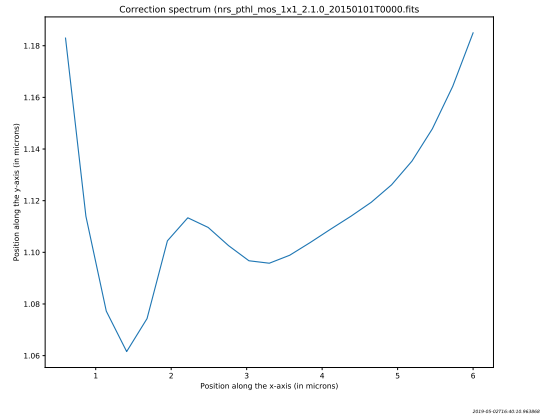
(e) FS400A1: Point-like source at 0.6  $\mu$  m



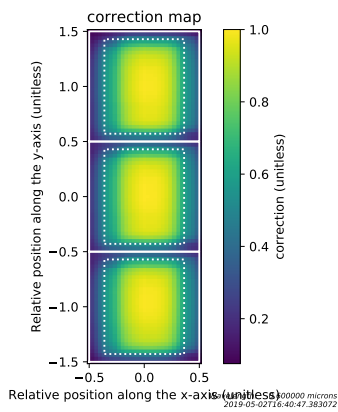
(f) FS400A1: Uniformly extended source



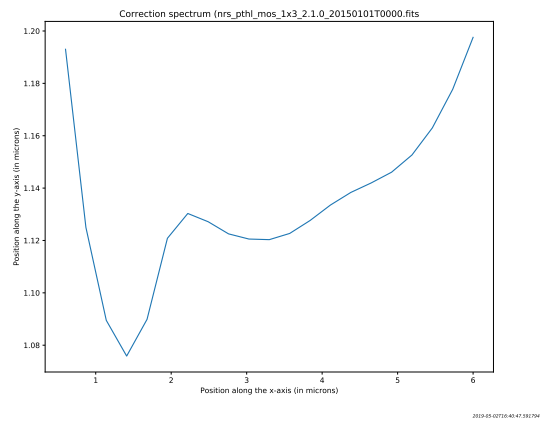
(g) MOS1x1: Point-like source at 0.6  $\mu$  m



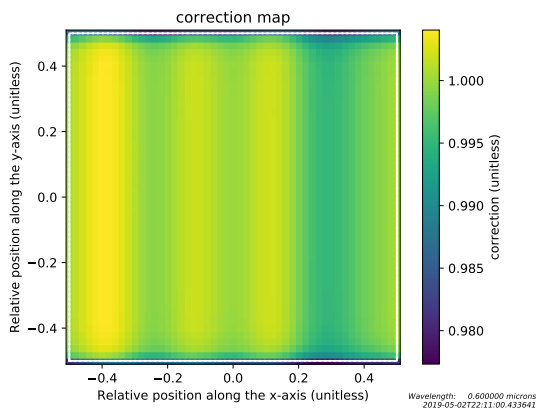
(h) MOS1x1: Uniformly extended source



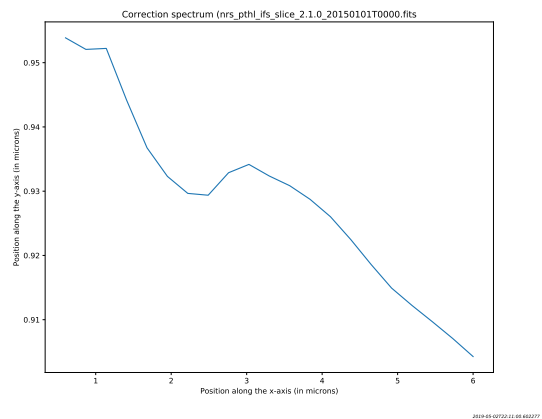
(i) MOS1x3: Point-like source at 0.6  $\mu$  m



(j) MOS1x3: Uniformly extended source



(k) IFS: Point-like source at 0.6  $\mu$  m



(l) IFS: Uniformly extended source

Figure 7: Path loss reference file extensions for NIRSpec observing modes and apertures

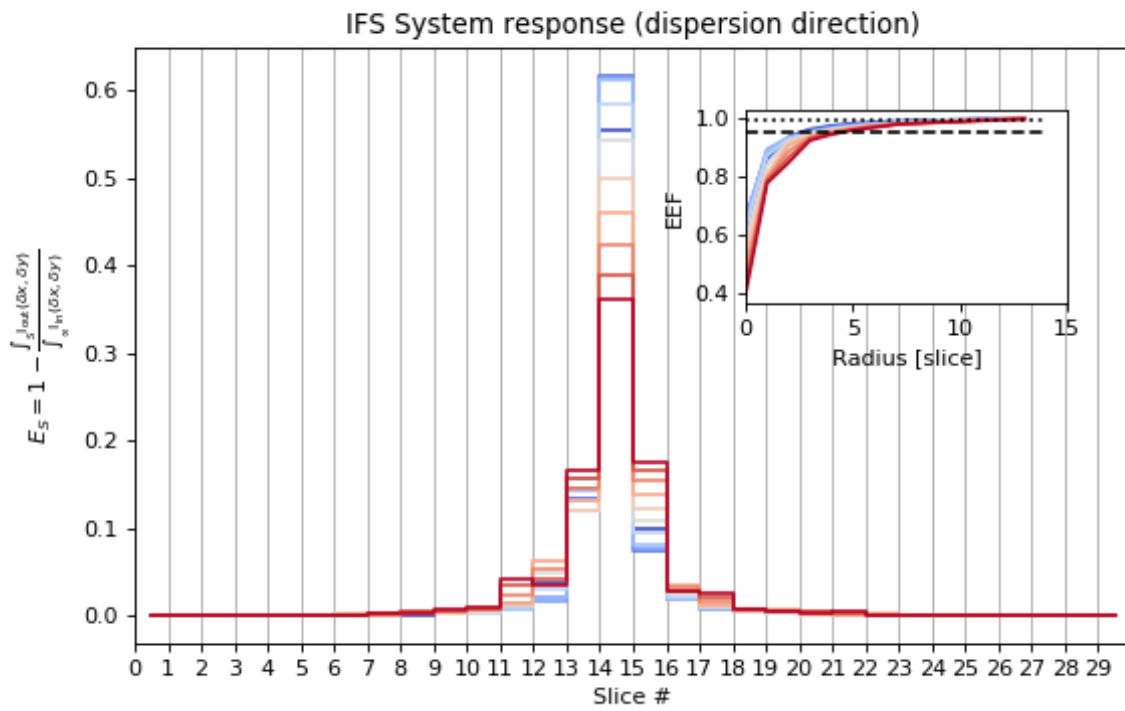


Figure 8: Simulated IFS system response at a sampling of one point per slice and associated EEF.

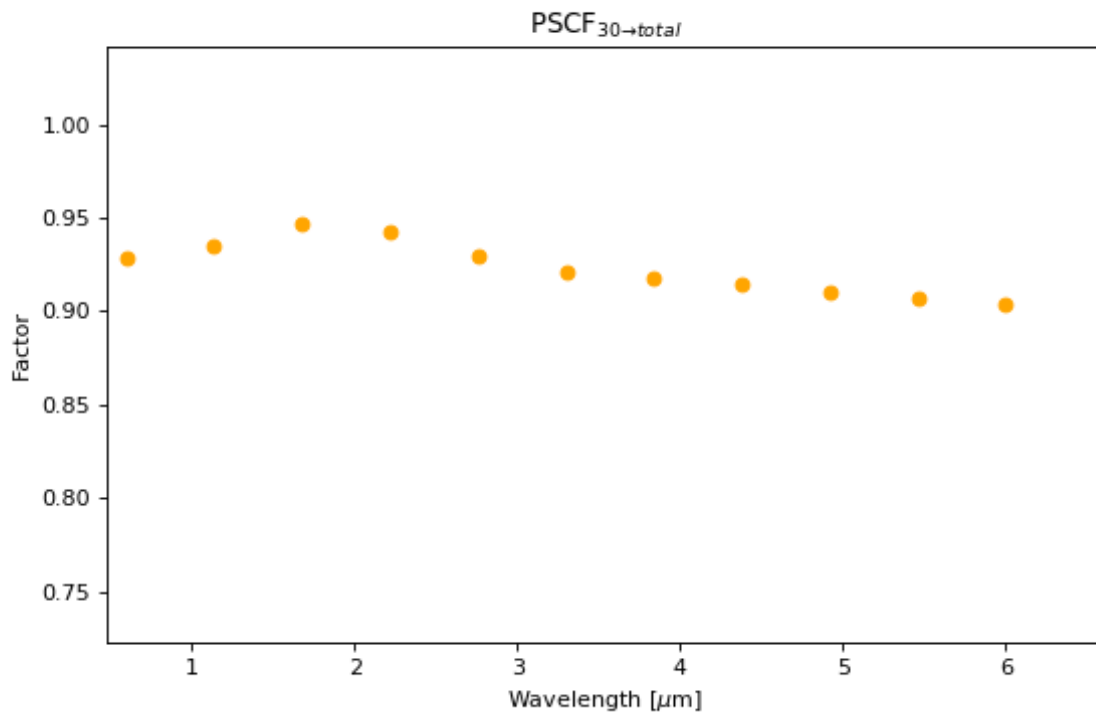


Figure 9: Fraction of the PSF falling in the IFS FoV (i.e. measured by the 30 slices).